Proceedings of the Ninth (1999) International Offshore and Polar Engineering Conference
Brest, France, May 30-June 4, 1999

ISBN 1-880653-39-7 (Set); ISBN 1-880653-40-0 (Vol. I); ISSN 1098-6189 (Set)

A 3D Boundary Element Code for the Analysis of OWC Wave-Power Plants

A. Brito-Melo and A.J.N.A. Sarmento
Instituto Superior Técnico
Lisbon, Portugal

A.H. Clément and G. Delhommeau
Ecole Centrale de Nantes
Nantes, France

ABSTRACT

This paper presents an application of a three-dimensional numerical code for modelling Oscillating Water Column (OWC) devices extended from a conventional radiation-diffraction code - AQUADYN - developed for the study of floating bodies. The problem is formulated in the frequency domain for infinite or constant finite depth and it is based on classical linear water wave theory and potential flow. The extension of AQUADYN to OWC systems requires a modification in the dynamic boundary condition on the internal water free surface to account for the imposed oscillatory pressure distribution within the chamber.

KEY WORDS: Oscillating Water Column, pressure distribution, added mass, damping coefficient, exciting force.

INTRODUCTION

The research and development work on wave energy utilisation through wave power plants of the OWC type, has been based much on analytical models. In this field we can find basic studies performed by several authors, of which we point out the work described by Evans (1982), Malmo & Reitan (1985) and Evans & Porter (1995). A significant contribution to the hydrodynamic modelling of OWC devices consisted in the introduction of the spatial variation of the internal free surface of the OWC chamber, by Falcão & Sarmento (1980), as opposite to the until then usual rigid piston approach. This theory was generalised by Evans (1982), and extended to a system composed of oscillating bodies and oscillating pressure distributions by Falnes & McIver, (1985). The mathematical modelling has been performed in mainly two-dimensions with simplified geometries, considering infinitely thin walls. As a result the final phases of plant design have been supported by laboratory tests with scale models. This experimental work has been mainly used to specify the appropriate design dimensions of the prototype (Ravindran et al, 1989, Joyce et al, 1993). Sarmento and Brito-Melo (1995) presented a 3D experimental-based mathematical model of the Azores OWC Pico power plant. This linear hydrodynamic model in the time domain is based upon experimental results obtained for this particular plant geometry, and so it does not allow to study effects related to a change in the geometry. Clement, (1996) used a two-dimensional numerical wave tank to compute the non-linear radiation step response of OWC wave-power plants and has investigated the influence of several geometric parameters. Three-dimensional panel codes based on the boundary element method, widely used for hydrodynamic applications, seem to be applicable to the case of oscillating water columns, provided that an appropriate boundary condition, which can account for the oscillatory pressure in the chamber, is applied in the internal water free surface. Lee et al (1996), describes a 3D panel method extended to an OWC device confirming that this approach is adequate to determine the hydrodynamic parameters affecting the design and performance of the system.

In the present study, we extend an existing diffraction-radiation 3D computational code – AQUADYN – developed at Laboratoire de Mecanique des Fluides, Ecole Centrale de Nantes (Delhommeau, 1987), to the study of floating bodies' hydrodynamics. In the modelling of the water column we apply the *direct approach*, where the dynamic boundary condition in the water free surface is modified to account for the applied pressure in the interior of the pneumatic chamber. This method, which follows the work of Lee et al (1996), will be described in detail and a comparison with the referred work will be presented, as well as tests of internal consistency to demonstrate the effectiveness and accuracy of the numerical code. The extended version of AQUADYN is applied to study the hydrodynamic performance of OWC systems by means of its hydrodynamic parameters and transfer functions. The present code is also used to analyse the performance of OWC devices with different geometric parameters, in order to demonstrate its usefulness as a tool in the design of OWC wave power plants.

HYDRODYMAMIC FORMULATION

Problem Statement

We consider the linear interaction of monochromatic waves with a 3D OWC device. This kind of wave energy device consists of an air chamber in which the front wall has an opening so as to let waves enter inside. The wave action makes the water level in the air chamber to oscillate and the air in the chamber is compressed and expanded generating an air flow through a turbine. A schematic sketch of this device is shown in Fig. 1. For the present study the structure is assumed to be at rest in a plane horizontal sea bottom at depth h. We take a Cartesian co-ordinate system with x, y horizontal, and z positive upwards, and the origin on the mean free surface, as shown in Fig. 1.

The fluid domain is bounded by the seabed at z=-h, the body surface, (S_b), the water free surface in the interior, (S_i), and exterior, (S_e), of the chamber and a cylindrical control surface sufficiently far away.

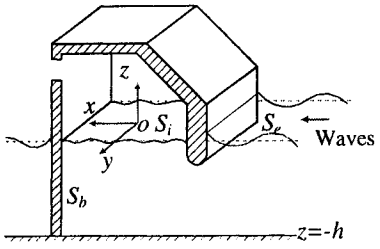

Fig. 1 3D schematic sketch of a bottom-standing OWC device.

According to the linear theory, when a sinusoidal wave interacts with a device of the OWC type, the pressure on the internal water free surface and the displaced flow, oscillate sinusoidally with the frequency , ω, of the incident wave. On the water free surface we wave the following pressure distribution:

$$P(x,y,z,t)-P_a=\begin{cases} pe^{-i\omega t} & ,\text{on } S_i \\ 0 & ,\text{on } S_e \end{cases}, \qquad [1]$$

P_a being the atmospheric pressure. The flow is considered irrotational and the fluid incompressible. The fluid motion is given by a complex velocity potential, $\phi(x,y,z)$, where the harmonic time dependence, $e^{-i\omega t}$ has been omitted and it must satisfy Laplace's equation everywhere in the fluid:

$$\nabla^2\phi=0 \ . \qquad [2]$$

In addition, it must satisfy certain boundary conditions, namely the following linearised boundary condition on the water free surface:

$$\frac{\partial\phi}{\partial z}-\frac{\omega^2}{g}\phi=\begin{cases} \dfrac{i\omega p}{\rho g} & \text{on } S_i \\ 0 & \text{on } S_e \end{cases}, \qquad [3]$$

where p is the complex amplitude of the oscillatory pressure acting on the internal free surface, g is the gravitational acceleration and ρ the water density. On solid boundaries the normal component of the fluid velocity must be equal to the velocity of the surface and this gives the following boundary conditions, respectively, on the surface of the body and on the sea-bed:

$$\frac{\partial\phi}{\partial n}=0 \ \text{ on } S_b, \qquad \left[\frac{\partial\phi}{\partial z}\right]_{z=-h}=0 \qquad [4]$$

The unit normal vector, n, on the body surface is defined pointing outwards from the body. Also a suitable radiation condition of outgoing waves at infinity distance is required for ϕ. Assuming linear theory the velocity potential may be decomposed in convenient three contributions, requiring that Eq. 2, 3 and 4 are satisfied:

$$\phi=\phi_o+\phi_d+\phi_R \ . \qquad [5]$$

This separation of the velocity potential is made so that $\phi_D=\phi_o+\phi_d$ is associated with the diffraction problem, where ϕ_o represents the undisturbed incident and ϕ_d the diffracted wave. The incident potential ϕ_o has the form:

$$\phi_o=-\frac{Ag}{\omega}e(kz)\cos[k(x\cos\beta+y\sin\beta)-\omega t] \qquad [6]$$

with $e(kz)=\dfrac{chk(z+h)}{chkh}$,

where β is the incident angle of the waves, A is the wave amplitude, h the water depth and k the wavenumber given from the dispersion-relation:

$$\omega^2=gk\tanh(kh) \ . \qquad [7]$$

The last component in Eq. 5 is the radiation potential due to the oscillating air pressure inside the chamber in otherwise calm waters and it can be expressed by the relation:

$$\phi_R=\frac{i\omega}{\rho g}p\phi_7 \qquad [8]$$

Here the potential ϕ_7 will be interpreted as the complex amplitude of the radiated velocity potential generated by an unit amplitude oscillatory pressure distribution. This concept is introduced by analogy with the one associated with the radiated waves due to each of the six body oscillation modes of a conventional floating body. In what follows, variables related to this problem will be denoted by the subscript 7.

This decomposition into elementary velocity potentials allow as to express the problem in terms of the diffraction and radiation problems, where it is necessary to solve a boundary value problem to, respectively, ϕ_d and ϕ_7. Therefore we have as follows:

Diffraction problem	**Radiation problem**
• the body-boundary condition:	
$\dfrac{\partial\phi_d}{\partial n}=-\dfrac{\partial\phi_o}{\partial n}$	$\dfrac{\partial\phi_7}{\partial n}=0$
• the sea-bed boundary condition:	
$\left[\dfrac{\partial\phi_d}{\partial z}\right]_{Z=-h}=0$	$\left[\dfrac{\partial\phi_7}{\partial z}\right]_{Z=-h}=0$
• the free-surface boundary condition:	
$\dfrac{\partial\phi_d}{\partial z}-\dfrac{\omega^2}{g}\phi_d=0$ on S_i, S_e	$\dfrac{\partial\phi_7}{\partial z}-\dfrac{\omega^2}{g}\phi_7=\begin{cases}1 & \text{on } S_i \\ 0 & \text{on } S_e\end{cases}$

Also the radiation condition of out-going waves at infinite distance is required for ϕ_d and for ϕ_7. We note that in the diffraction problem, as we assume that the chamber is held fixed and open to the atmosphere, the corresponding boundary equations are the same as for a floating body. The formulation for the radiation problem in terms of a potential ϕ_7 allows us to extend a conventional code developed for the analysis of floating bodies with six degrees of freedom to the OWC system. This is done by taking the pressure distribution oscillation as a seventh degree of freedom. For a conventional floating body the

hydrodynamic force in the j-th direction due to a unit amplitude motion of each mode is evaluated by carrying out direct pressure integration over the wetted body surface, given by the following expression:

$$F_j = i\omega\rho \iint_{S_b} \phi n_j dS \ , \qquad [9]$$

This definition is extended to the present application - the OWC system - by defining a global surface (S_b+S_i), which is the body surface plus the internal water free surface and by introducing a normal component, n_7, so that:

$$n_7 = \begin{cases} 1 & \text{on } S_i \\ 0 & \text{on } S_b \end{cases} \ . \qquad [10]$$

Extending the concept of hydrodynamic force to this global surface it comes out:

$$F_7 = i\omega\rho \iint_{S_i} (\phi_o + \phi_d + \frac{i\omega\, p}{\rho g}\phi_7) n_7 dS \qquad [11]$$

where the component

$$X_7 = i\omega\rho \iint_{S_i} (\phi_o + \phi_d) n_7 dS \ , \qquad [12]$$

corresponds to the exciting force (resulting from an incident wave in a chamber open to the atmosphere). The integral of the last term corresponds to the radiation force component and it is frequently expressed in terms of the added mass, A_7, and damping, B_7, coefficients associated with the pressure distribution problem. These coefficients can be expressed by the following relations:

$$A_7 = \rho\, \mathrm{Re}\left[\iint_{S_i} \phi_7 n_7 dS\right] , \qquad B_7 = \rho\omega\, \mathrm{Im}\left[\iint_{S_i} \phi_7 n_7 dS\right] .$$

By applying the Haskind relation, we can relate the damping coefficient B_7 with the exciting force component, as follows:

$$B_7 = \frac{k}{8\pi\rho g A^2 C_g} \int_0^{2\pi} |X_7(\beta)|^2 d\beta \ . \qquad [13]$$

In this expression X_7 is integrated with respect to the wave incident direction, β, and C_g represents the group velocity.

We may emphasise that the concepts of hydrodynamic forces, radiation coefficients and exciting forces reported here are applied to the OWC system as a mathematical extension of expressions developed in the floating bodies context. However, the concept of excitation force on a fixed rigid-body is associated with the excitation volume-flux, that is, the air flux displaced by the internal water surface due to an incident wave when the chamber is at atmospheric pressure. The modes of rigid-body motion, where the corresponding normal velocity is specified on the body surface, are associated with the displacement of volume in the chamber of the OWC device due to an imposed pressure oscillation on the internal water free surface. The total flow displaced by the wave inside the air chamber can be expressed as the sum of the radiation and diffraction flows, respectively given by:

$$Q_R = \frac{i\omega p}{\rho g} \int_{S_i} \frac{\partial \phi_7}{\partial z} dS \ , \qquad [14]$$

$$Q_D = \int_{S_i} \frac{\partial(\phi_d + \phi_o)}{\partial z} dS \ . \qquad [15]$$

According to linear theory, the interactions between waves and the OWC device may be represented by transfer functions in the frequency domain. The diffraction flow may be related to the incident wave elevation, A, at the point (x_0, y_0), by means of a diffraction transfer function:

$$H_D(\omega; x_0, y_0) = \frac{Q_D(\omega)}{A(\omega; x_0, y_0)} \ . \qquad [16]$$

The radiation flow can also be related with the derivative of the air pressure inside the chamber. This relation is expressed in the frequency domain by the radiation transfer function:

$$H_R(\omega) = -\frac{Q_R(\omega)}{i\omega P(\omega)} \qquad [17]$$

In the time domain these relations are represented by the inverse Fourier transforms of the transfer functions, the real impulse response functions.

Integral Equations

The boundary-value problem is solved by using a direct zeroth-order Boundary Element Method (BEM). The potential is obtained as a solution of integral equations by the use of Green's theorem. The velocity potential may be represented in terms of a normal dipole distribution of density $\mu = -\phi$, and a source distribution of density $\sigma = \frac{\partial \phi}{\partial n}$, by choosing the internal potential to be zero. The second identity of Green is applied in the surface comprised by the mean wetted body surface, the water free surface in the interior and exterior of the chamber, the seabed and the control surface. Considering the two problems of diffraction and radiation, separately, and entering in consideration with the boundary equations the following integral equations can be obtained:

$$\frac{\phi_d(M)}{2} - \frac{1}{4\pi} \iint_{S_b} \phi_d(M') \frac{\partial G}{\partial n} dS(M') = -\frac{1}{4\pi} \iint_{S_b} \frac{\partial \phi_d(M')}{\partial n} G dS(M') \qquad [18]$$

$$\frac{\phi_7(M)}{2} - \frac{1}{4\pi} \iint_{S_b} \phi_7(M') \frac{\partial G}{\partial n} dS(M') = -\frac{1}{4\pi} \iint_{S_i} G dS(M') \qquad [19]$$

where M' represents a point (x',y',z') where the integration is performed, M is the influence point (x,y,z) and $G(M',M)$ is the Green's function satisfying boundary conditions on the water free surface, on the bottom and the radiation condition at infinity.

Here we emphasize the fact that the integral equation of the diffraction problem in the OWC system is the same as for the case of a conventional floating body. However, for the radiation problem, on the right side of eq. 19, we have the integral of Green's function over the internal water free surface instead of the one integrated on the surface of the body.

Numerical resolution

To obtain the numerical solution of the above equations we approximate the integrals over the surfaces, by a summation of integrals over all the elements that discretize the surfaces. This method of solution involves discretizing the surface, S_b, into N panels and S_i into M panels and assuming the potential to be constant on each panel. When writing the integral equations, eqns. 18 and 19 on the control point selected as the centroid of each panel, we obtain a system of linear equations, respectively, for the diffraction and the radiation problem:

$$\sum_{j=1}^{N} \mu_{d_j} D_{ij} = -\sum_{j=1}^{N} \sigma S_{ij} \qquad [20]$$

$$\sum_{j=1}^{N} \mu_{7_j} D_{ij} = -\sum_{j=1}^{M} S_{ij} \; . \qquad [21]$$

where S_{ij} and D_{ij} are the influence coefficients of the Green's function, defined by its integral or the integral of its normal derivative (respectively) over an element. The sources are known from the body condition and the normal dipoles are the unknowns, i.e. the solution of each problem.

To illustrate the computation of the influence coefficients we may consider a general case expressing a coefficient as a sum of two terms C_1 and C_2: the first one is given by the integral of a function of $1/R$ (in which R designates the distance between a point M and M') over an element, Se); The second term is given by the integral over an element of an integral in θ:

$$C_1 = \iint_{Se} f\left(\frac{1}{R}\right) dS(M') \qquad C_2 = \iint_{Se} \left[\int_{-\pi/2}^{\pi/2} g(M',\theta) d\theta \right] dS(M')$$

The initial version of AQUADYN calculates analytically the term C_1 by classical Hess and Smith (1966) formulas and uses the asymptotic formulation for pair of elements where the distance between each other is high when comparing to the panel dimension over which the integration is performed. For the term C_2 AQUADYN perform first the integral in θ by interpolation into a file where the integral is tabulated in terms of four elementary functions of two variables. Then the spatial integration over the element is evaluated by using a 1-point Gaussian integration method.

When extending the original code to the OWC system, particular attention must be paid to the calculation of the term C_2. We notice that the analytical formulation is required to compute the spatial integration when $M=M'$ and $z=0$, that is, on the internal water free surface, as we saw that the asymptotic formulation diverges for these cases. Another point is related with the particular geometric configuration of the OWC system and the thickness of the walls. The 1-point Gaussian integration method revealed good accuracy in the case of floating body analysis. However in some particular OWC geometries this method may fail to give satisfactory results, in particular near the resonance.

NUMERICAL RESULTS

The extended AQUADYN version was first validated with published case tests. In this paper we present, for illustration, a comparison of the present code with the one applied by Lee et al, (1996), designed by WAMIT. This study concerns the case of a fixed square moon pool in waters of infinite depth and an OWC device with a harbour in front of the chamber, in waters of finite depth, these two cases are represented in Fig. 2a and 2b. The same direct method was used in both codes.

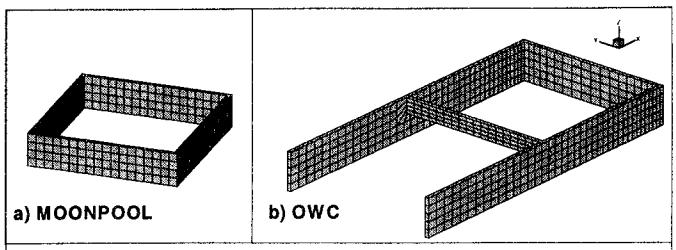

Draft: 5.0 m
Horizontal dimensions: 20.0 x 20.0 m
Walls thickness: 0.5 m
Front wall submerged aperture on the OWC: 3.0 m
Length of the harbour of the OWC: 20.0 m

Fig. 2 a) Discretization of a square moon pool in waters of infinite depth and b) an OWC with a harbour mounted on the sea bottom

Figure 3 shows the results of the comparison of the two codes concerning the dimensionless damping coefficient, B_7, against dimensionless wave number kL (L=10.0 m, L is half the length of the chamber), in order to validate AQUADYN for a simple structure in infinite depth. We observe that the piston mode is resonant near kL=1.0 for both codes and the agreement between results from the two codes is satisfactory, improving for larger wavenumbers. Fig. 3 also presents a comparison between the results from AQUADYN computed with 1-point Gaussian method with the body and the water free surface discretized, respectively, in N=336 and M=72 elements, with a more refined discretization with N=540 and M=210 panels. The 1-point Gaussian method is also compared with the analytical integration. For this geometry the convergence is achieved with a small number of panels and the solution of the linear system is not sensible to errors introduced in the influence coefficients matrix, since the 1-point gives the same result as the analytical integration.

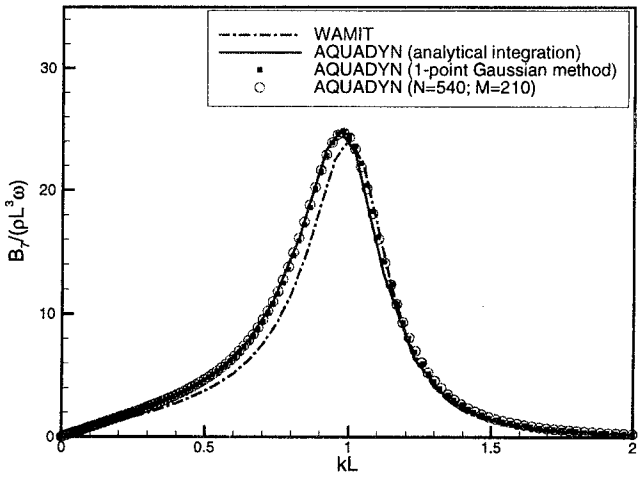

Fig. 3 Non-dimensional damping coefficient, B_7, for the moon pool geometry

For an OWC system the problem can be ill-conditioned near the resonance, as it is refereed in Lee et al, and this fact becomes more relevant in structures with walls of small thickness. In order to verify the behaviour of the condition number of the coefficients matrix with the wall thickness, we performed this calculation for the case of the moon pool near the resonance frequency. The condition number was computed by applying the singular value decomposition technique (SVD). As it was expected, as the wall thickness decreased the

coefficients matrix became ill-conditioned. For this particular structure with 0.5 m of thickness, the matrix is well-conditioned.

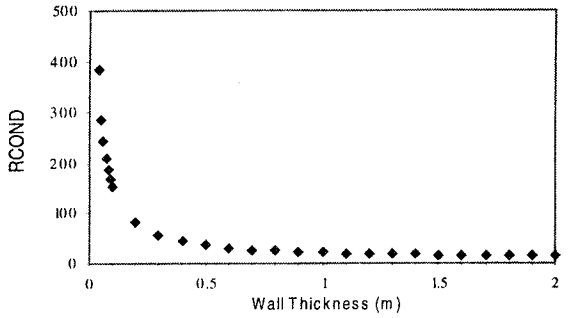

Fig. 4 Condition Number, RCOND, of the influence coefficients matrix for the case of the moon pool with varying wall thickness.

For the OWC system represented in Fig.2b, the results of the comparison between AQUADYN and WAMIT concerning the dimensionless damping coefficient, B_7, the cross-coupling added mass A_{17} and damping B_{17} coefficients against dimensionless wave number kL (L=10.0 m) are represented in Fig. 6. These results were obtained with 1132 panels, corresponding to the medium discretization used by WAMIT, whereas the internal water free surface was meshed into 414 panels. We see good agreement between the results from the two codes and the major errors were observed near the resonant wavenumber. For this particular structure a 4-point Gaussian method was used. It was found that with a 1-point method the solution did not agree with the results from WAMIT. The convergence between 1-point and 4-point method was not reached even if the discretization was much more refined. No significant difference was found between results with 9 and 4 points in the Gaussian method.

For this device it was verified that the solution of the linear system was highly sensitive to errors in the computation of the influence coefficients. We found a condition number of 2000 for this matrix, near the resonance frequency, which correspond in simple precision to about 3 significative digits for the solution. In Fig. 5 we represent the condition number of the influence coefficients matrix for varying wave numbers. As we can see the matrix becomes more ill-conditioned near the resonant wavenumber. These structures may require a more accurate method for the computation of the influence coefficients, particularly near the resonance. We found that the major errors in the influence coefficients occur between the panels on the intersection of the lateral wall with the partially submerged front wall and the adjacent panels on this wall. Smaller errors are found between nearly panels existing in opposite sides of a wall. These errors can affect significantly the results in plants with long harbour walls, since in this case the number of panels in this situation increases significantly.

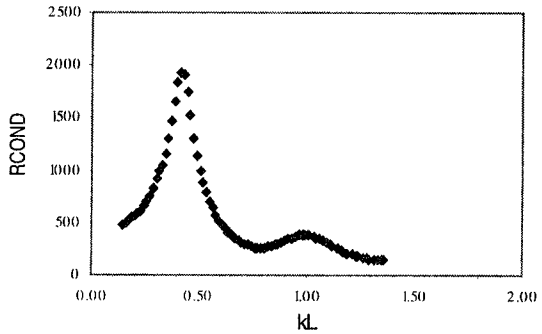

Fig. 5 Condition Number of the coefficients matrix for the case of OWC with an harbour with varying the dimensionless wavenumber.

By carrying out numerical computations with varying wall thickness of this structure, it was observed that, as the thickness of the structure increases, the solution of the linear system obtained with 1-point Gaussian method approaches the one obtained with the 4-point method, as it was expected. However we do not get exact convergence between these two methods and we observe that the condition number does not depend only on the walls thickness. This suggest that influence coefficients from panels in the intersection of the front wall with the lateral wall and adjacent panels in the front wall are responsible for the ill-conditionement.

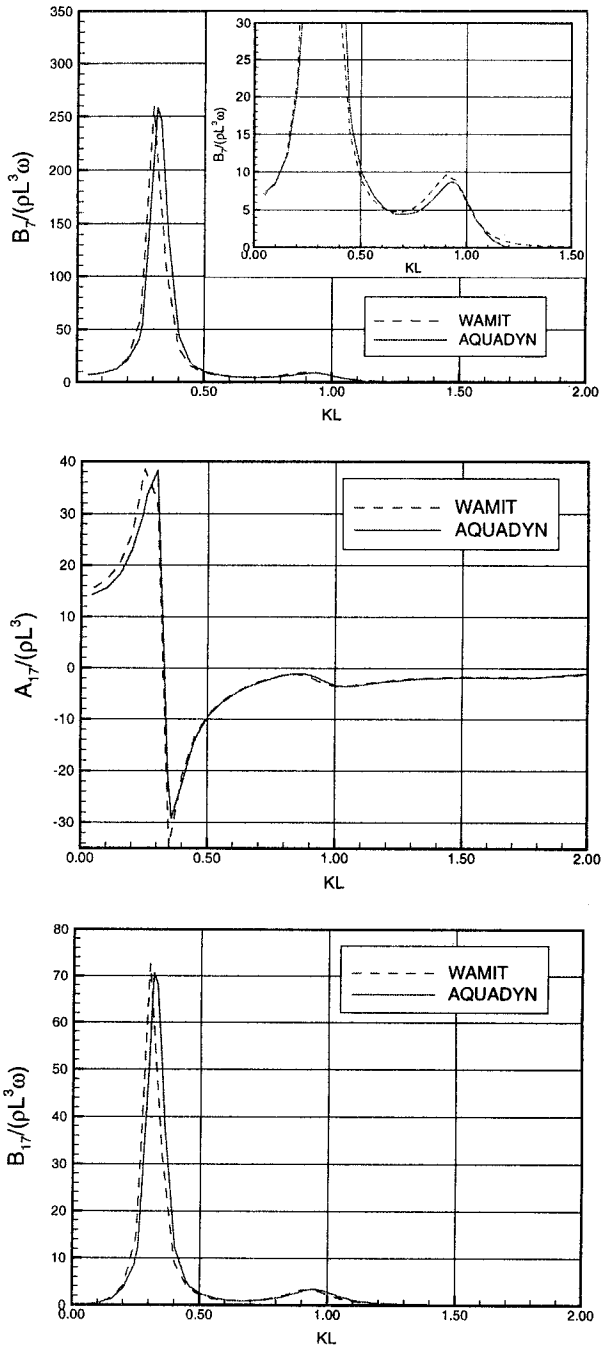

Fig. 6 Non-dimensional damping coefficient B_7 and cross-coupling added mass A_{17} and damping B_{17} coefficients

Next we present the numerical results for an OWC device geometry with a configuration identical to the one at Pico Plant in the Azores. The configuration of this device and its mesh are presented in Fig. 7, corresponding to N=1567 panels. The internal water free surface was discretized into 506 panels. Numerical tests showed that with this discretization the convergence of the results at different periods is obtained. Convergence tests with 1 and 4 point's gaussian method indicated that good accuracy results could be obtained with only 1 point. Yet, we point out the fact that a bigger thickness was considered in this structure.

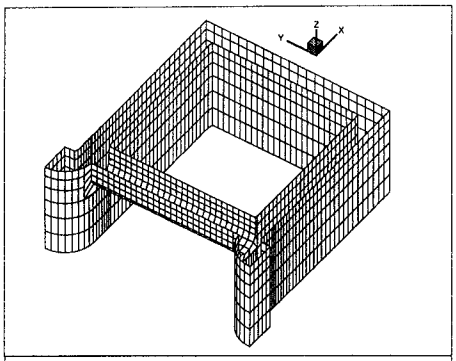

Draft:7.8 m
Horizontal dimension:12x12 m
Front wall thickness: 2.0 m
Other Walls thickness: 1.5 m
Front wall aperture: 5.3 m

Fig. 7 Discretization of the OWC device

A test to the agreement between the radiation and diffraction problems can be made by comparing the values of the damping coefficient, B_7, calculated from the direct method and from the Haskind relation, as presented in Fig. 8. This comparison was used to test the convergence of the numerical calculation.

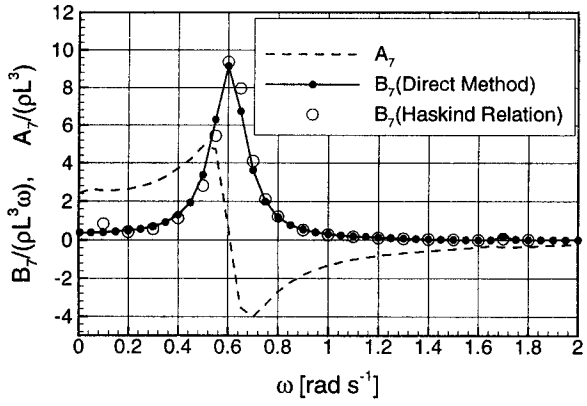

Fig. 8 Non-dimensional Added Mass and Damping coefficients.

The added mass and damping coefficients are non-dimensionalised, respectively, by ρL^3 and $\rho L^3 \omega$, with $L = 12.0\,\mathrm{m}$. We can see that there is a good agreement between the results from the radiation and the diffraction problems.

Diffraction Problem

The diffraction problem can be analized through the behaviour of the diffraction transfer function (Eq 16), as represented in Fig. 9. We observe three peaks of resonance, the first one at ω=0.62 rad/s and the second one at ω=1.68 rad/s. After the third peak the function is negligible.

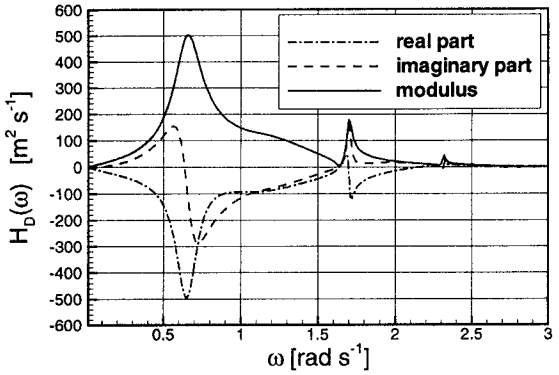

Fig. 9 Diffraction transfer function.

Figs. 10a and 10b depict a top view of the inner OWC free surface showing the spatial variation of the modulus of the vertical velocity for those two peak frequencies. We can see that for the first peak of resonance the velocity field inside the chamber is uniform, corresponding to a piston mode; in the second peak we observe zero velocities in the centre of the chamber, with increasing velocities (in modulus) towards the front and backward walls, thus corresponding to a sloshing mode.

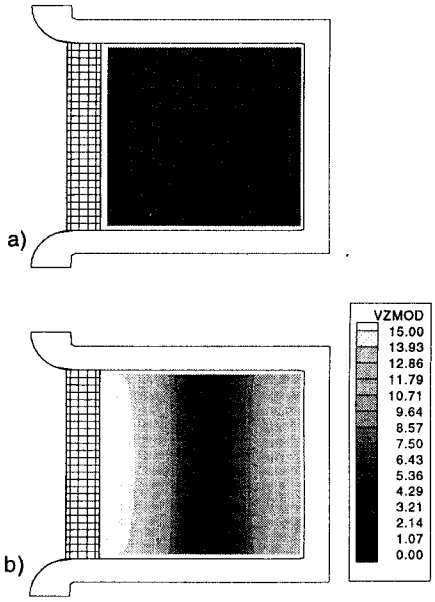

Fig. 10 Velocity field modulus in z-direction for frequencies of 0.62 rad/s (a) and 1.68 rad/s (b).

The variation of the exciting force modulus with wave angle of incidence is plotted in Fig. 11 for the case of these two frequencies. As

might be expected, for the first peak of resonance, the exciting force reaches its maximum for zero wave incidence and decreases monotonically as the incident wave angle increases to π rad. For the second peak of resonance the average water motion inside the chamber reduces to almost zero for an incident angle a bit less than $3\pi/4$ and then increases as the angle goes to π (i.e. as the incident wave comes from the backside).

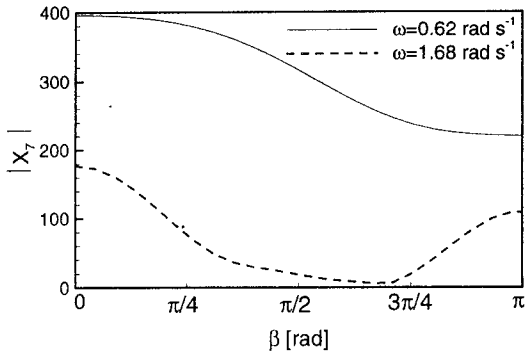

Fig.11 Variation of the exciting force modulus with incident wave direction for wave frequencies of 0.62 rad/s and 1.68 rad/s.

To compute the diffraction transfer function showed in Fig. 9 we set the reference point in $(x,y)=(0,0)$ (see Fig. 1); if we perform the inverse Fourier transform of this function, the impulse function will come out (solid line in Fig. 12). We can see from this figure that $h_d(t)$ is a non-causal function (i.e. $h_d(t) \neq 0$, $t<0$). This means that the chosen input (the water elevation at point (0,0)) is not the cause of the output. The non-causality of this function has been discussed by Falnes, (1995).

To obtain an indication on how far "upstream" the incident wave elevation should be measured in order to make the corresponding impulse response function approximately causal, we computed this function with different reference points on the upstream outside the body. In Fig. 12 we can see that, for this particular device, it will be necessary to measure the incident wave elevation at a position x_0=-40 m, in order to be able to determine the present-time diffraction flow with reasonable approximation, without requiring future values of the water elevation to be known. This result can be useful in implementing on-line optimal control schemes of the wave power plant.

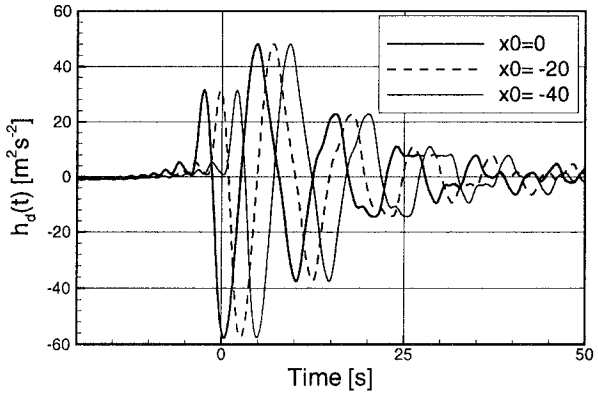

Fig. 12 Impulse response function of diffraction problem for several upstream measurements points (x_0 in metres).

Radiation problem

The radiation transfer function is represented in Fig. 13, on top; on the bottom we can see its inverse Fourier transform, the impulse response function of the pressure radiation problem, $h_r(t)$. We confirm that this function is null for negative values of its argument, in agreement with the expected causality of this function (i.e. the fact that no air flow occurs prior to the forcing pressure action). As expected the peaks of the radiation transfer function occur for the same frequency as in the diffraction problem.

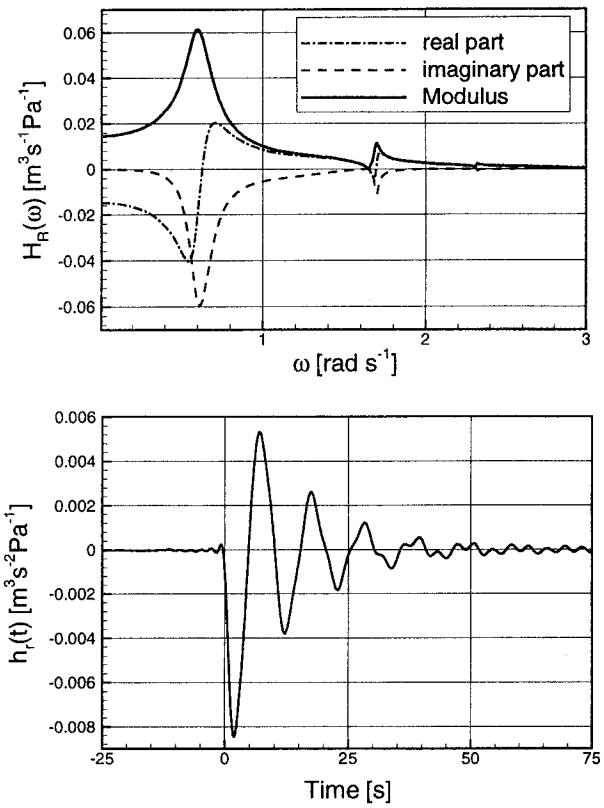

Fig. 13 Transfer function (above) and Impulse response function (below) of the radiation problem.

Influence of geometrical parameters

The characteristics of resonance are important in the design of OWC devices. AQUADYN extended version can be used as a tool for the analysis of the influence of the geometrical parameters on the hydrodynamic performance of the OWC device. As an example, here we present results for the effect of increasing the front wall submergence depth, from 2.5 m (geometry of Fig. 7) to 5.0 m, on the hydrodynamic damping coefficient, while the other parameters are the same as in the previous calculation. Fig. 14 (on top) shows the curves of B_7 for different front wall submergence depths, h, against non-dimensional wave number kL (L=12.0 m).

We notice an increase and narrowing of the peak as the front wall submergence varies from 2.5 m to 5.0 m, and the resonance peak shifts to lower frequencies. The reduction of the resonance frequency and the narrowing of the curve are related to the increase in the mass of the oscillating water column as the front wall submergence increases as shown in Fig. 14 (below).

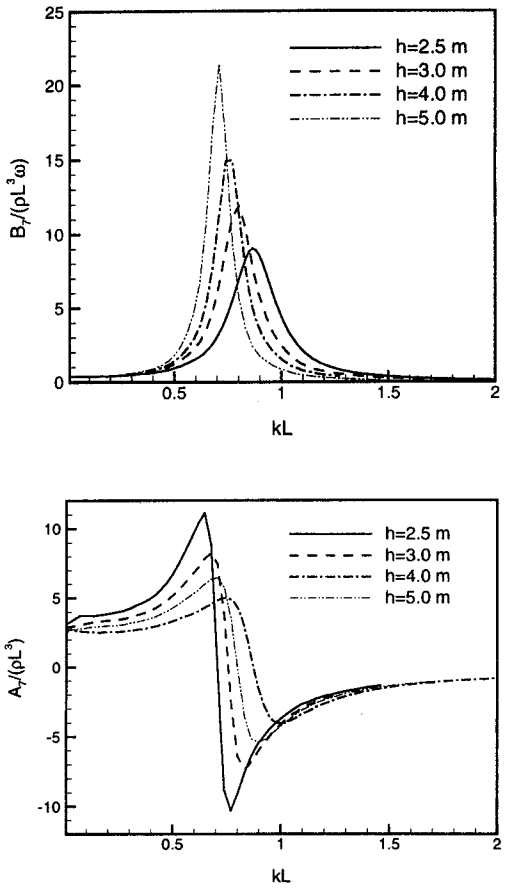

Fig. 14 Dimensionless damping (above) and added mass (below) coefficients for different front wall submergence depths, *h*.

CONCLUSION

This work deals with a method to adapt a numerical code, used in the analysis of conventional floating bodies, to the OWC system. The extended code has been well validated with published test cases and the results obtained confirmed that the used method is able to accurately predict the hydrodynamic behaviour of wave power plants of this type.

The code has been also applied for the geometry of the Pico plant device. Several relations between the hydrodynamic parameters have been checked, namely the Haskind relation. The numerical evaluation of the impulse response functions of the diffraction and radiation problems was performed. These functions, closely related to the geometry of the device, were found to be consistent with theoretical studies. Computation of the velocity field on the water free surface for resonance frequencies showed that the first resonance frequency corresponds to a piston mode and the second one to a sloshing mode. The numerical code was used to analyse the effect of changing the front wall submergence depth and the results obtained were in agreement with theoretical expectations.

A detailed analysis of the influence coefficients matrix of the linear system was performed near the resonance frequency, where the discrete problem is ill-conditioned. The limitation of the 1-point Gaussian method used in the initial version of AQUADYN applied to floating bodies, was pointed out for the case of OWCs devices. It was verified that this method is accurate for larger walls thickness but it can fail with decreasing thickness, since the influence coefficients matrix of the linear system became ill-conditioned. The increase in the number of gaussian points from one to four in the numerical integration method can be enough to improve the numerical precision in the computation of hydrodynamic coefficients.

ACKNOWLEDGEMENTS

The authors acknowledge the Franco-Portuguese Corporation project number N3/03P. This work was undertaken under contract number PRAXIS/3/3.1/CEG/2634/95 and JOULE JOR3-CT95-0012.

REFERENCES

Clément, A. H. (1997).'Dynamic Nonlinear Response of OWC Wave Energy Devices', *International Journal of Offshore and Polar Engineering*, Vol. 7, No. 2., pp 91-96.

Delhommeau, G. (1987).'Les problèmes de diffraction-radiation et de résistance de vagues: étude théorique et résolution numérique par la méthode des singularités' – *Thèse de Docteur ès Sciences*, E.N.S.M. Nantes.

Evans, D. V. (1982).'Wave-power absorption by systems of oscillating surface pressure distributions'. *J. Fluid. Mech.* 114, 481-99.

Evans, D. V. & Porter, R. (1995). 'Hydrodynamics characteristics of an oscillating water column device', *Appl. Ocean Research* 17, pp 155-164.

Falcão, J. & Sarmento, A.J.N.A. (1980). 'Wave generation by a periodic surface pressure and its application in wave-energy extraction'. *15th Int. Cong. Theor. Appl. Mech.*, Toronto.

Falnes, J. & McIver, P. (1985). 'Surface wave interactions with systems of oscillating bodies and pressure distributions'. *Appl. Ocean Research.* Vol.7, No. 4, pp. 225-234.

Falnes, J. (1995). 'On non-causal impulse response functions related to propagating water waves' *Appl. Ocean Research,* Vol. 17, pp. 379-389.

Joyce, A.; J. Bettencourt; T. Pontes; A. Sarmento; L. Gato e A. F. de O. Falcão; Brito-Melo, A. (1993).."Wave Tank Testing of a Shoreline OWC Power Plant", *Proc. of the European Wave Energy Symposium.*

Lee, C.-H., Newman, J.N. and Nielsen, F.G. (1996). 'Wave Interactions with an Oscillating Water Column', *Proc. of the 6th Int. Offshore and Polar Eng. Conf.*, Los Angeles, ISOPE, Vol I, pp 82-90.

Malmo, O. & Reitan, A. (1985). 'Wave-power absorption by an oscillating water column in a channel' , *J. Fluid. Mech.*, vol. 158, pp. 153-175.

Ravindran, M. & Swaminathan, G. (1989). ' Model Studies for the sea trial of a 150 kW wave energy system'. *Presented at the 8th Int Conf. on Offshore Mechanics and Arctic Eng.,* The Hague – March 19-23.

Sarmento, A.J.N.A. and Brito-Melo, A. (1995). 'An Experiment-Based Time-Domain Mathematical Model of OWC Power Plants', *Int. J. Offshore and Polar Engng.*, Vol. 6, No.3, pp. 227-233.